

Axionic quantum criticality of generalized Weyl semimetals

Gabriel Malavé,¹ Rodrigo Soto-Garrido,¹ Vladimir Juričić,² and Bitan Roy³

¹*Facultad de Física, Pontificia Universidad Católica de Chile,
Vicuña Mackenna 4860, Santiago 8331150, Chile*

²*Departamento de Física, Universidad Técnica Federico Santa María, Casilla 110, Valparaíso, Chile*

³*Department of Physics, Lehigh University, Bethlehem, Pennsylvania, 18015, USA*

We formulate a field theoretic description for d -dimensional interacting nodal semimetals, featuring dispersion that scales with the linear (n th) power of momentum along d_L (d_M) mutually orthogonal directions around a few isolated points in the reciprocal space with $d_L + d_M = d$, and residing at the brink of isotropic insulation, described by N_b -component bosonic order parameter fields. The resulting renormalization group (RG) procedure, tailored to capture the associated quantum critical phenomena, is controlled by a ‘small’ parameter $\varepsilon = 2 - d_M$ and $1/N_f$, where N_f is the number of identical fermion copies (flavor number). When applied to three-dimensional interacting general Weyl semimetals ($d_L = 1$ and $d_M = 2$), characterized by the Abelian monopole charge $n > 1$, living at the shore of the axionic insulation ($N_b = 2$), a leading order RG analysis suggests Gaussian nature of the underlying quantum phase transition, around which the critical exponents assume mean-field values. A traditional field theoretic RG analysis yields same outcomes for simple Weyl semimetals ($n = 1$, $d_L = 3$, and $d_M = 0$). Consequently, emergent marginal Fermi liquids showcase only logarithmic corrections to physical observables at intermediate scales of measurements.

Introduction. Fermi liquids, prominent itinerant electronic systems, host gapless sharp fermionic excitations around closed contours in the momentum space, known as Fermi surfaces [1]. In the presence of electronic interactions, they become unstable toward charge-density-wave, ferromagnet, antiferromagnet, and nematicity [2–8], for example, ultimately giving away to superconductivity at the lowest temperature [9–11]. These orderings set in through quantum phase transitions (QPTs), yet their controlled field theoretic description remains challenging due to an infinite number of fermionic nodes in the system, coupled to critical bosonic fluctuations.

Nodal Fermi liquids also feature gapless fermionic excitations, but around a few special points in the Brillouin zone. Besides showcasing novel topological responses [12], they constitute a key testbed for itinerant quantum critical properties. Dirac and Weyl liquids, with the chemical potential pinned at the band touching points at half-filling, are their prime candidates. The linear energy-momentum relation, endowing the elegant Lorentz invariance, allows traditional field-theoretic renormalization group (RG) techniques to capture the underlying quantum criticality therein [13–23]. In parallel, field-theoretic predictions can be tested from infamous sign-problem-free quantum Monte Carlo simulations [24–32]. Fascinatingly, these methodologies apply to some open or non-Hermitian Dirac systems [33–35].

However, established RG techniques are inadequate when topological semimetals display *nonlinear* dispersion along certain high symmetry directions due to the lack of Lorentz symmetry [36]. This is the case in Weyl semimetals (WSMs) with the underlying Weyl nodes characterized by Abelian monopole charge $n > 1$, a family of systems at the central focus in this article, hereafter named general WSMs. The fermionic dispersion therein

is linear along the direction connecting two Weyl nodes (k_z), while in the perpendicular plane it scales as k_\perp^n , where $\mathbf{k}_\perp = (k_x, k_y)$ [37–41]. Vanishing density of states $\rho(E) \sim |E|^{2/n}$ around the Weyl nodes protects them against sufficiently weak electron-electron interactions. Nevertheless, an axionic insulator emerges as the dominant ground state for strong repulsive electronic interactions, in which two Weyl nodes get coupled and the translational symmetry is broken spontaneously [42–46].

Here, we develop a general field-theoretic RG approach to capture the quantum critical behavior of a d -dimensional semimetal, in which the fermionic dispersion scales with the linear (n th) power of momentum along d_L (d_M) mutually orthogonal directions, with $d_L + d_M = d$, near a QPT to an insulator, described by an N_b -component bosonic order-parameter field. Naturally, this procedure encompasses a three-dimensional (3D) general WSM ($d_L = 1$ and $d_M = 2$) to an axionic insulator ($N_b = 2$) QPT. The proposed RG approach is controlled by a ‘small’ parameter $\varepsilon = 2 - d_M$ and $1/N_f$, where N_f is the number of identical fermion copies (flavor number). From a leading-order RG analysis we find that such a QPT in any general WSM is Gaussian in nature. For conventional WSM ($n = 1$ and $d_L = 3$), we arrive at this conclusion from the existing RG procedure. Thus, the critical exponents, which ultimately assume their mean-field values, only *logarithmically* influence the scaling of various physical observables at intermediate scales (temperature or frequency) of measurements in the emergent critical marginal Fermi liquids.

Model. The effective single-particle Hamiltonian describing such a non-interacting nodal-point semimetal is

$$H_0(k_i) = \sum_{l=1}^{d_L} v_l \Gamma_l k_l + \sum_{n=1}^{d_M} \Gamma_{d_L+n} \varepsilon_n (k_{d_L+1}, \dots, k_d), \quad (1)$$

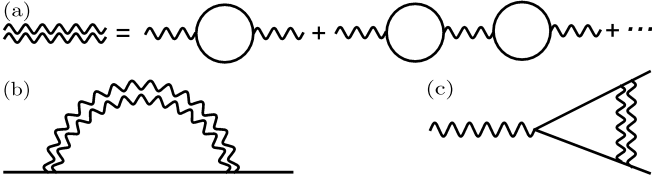


FIG. 1. (a) Feynman diagram representation of the dressed boson propagator (double wavy line) resulting from the random phase approximation processes, where the solid (single wavy) line correspond to fermion (bare boson) propagator. Feynman diagrams for (b) fermionic self-energy and (c) Yukawa vertex corrections through dressed boson propagator.

where k_i are the components of momentum, $\{\Gamma_i\}$ is a set of mutually anticommuting Hermitian matrices, satisfying $\{\Gamma_i, \Gamma_j\} = 2\delta_{ij}$, ε_n are non-linear functions of their

$$S = \sum_{p=1}^{N_f} \left[\int_k \psi_{p,k}^\dagger G_0^{-1}(k) \psi_{p,k} + \frac{g_0}{\sqrt{N_f}} \int_{k,q} \phi_q \cdot \psi_{p,k+q}^\dagger \Upsilon \psi_{p,k} \right] + \frac{1}{2} \int_q D_0^{-1}(q) \phi_{\bar{q}} \cdot \phi_q + \frac{u_0}{2} \int_{k,q,q'} \phi_{\bar{q}} \cdot \phi_{q+q'} \phi_{\bar{k}} \cdot \phi_{k-q'}, \quad (2)$$

where $\bar{x} = -x$, $k = (k_0, k_1, \dots, k_d)$, with k_0 being the Euclidean frequency, while $\psi_{p,k}$ (ϕ_q) represents the p th copy (real vector) of the Grassmann (order parameter) field. The bare Yukawa (ϕ^4) coupling is g_0 (u_0). Here, we consider N_f identical copies of fermions. The bare fermionic and bosonic propagators are given by

$$G_0(k) = [ik_0 + H_0(k_1, \dots, k_d)]^{-1}, \quad (3)$$

$$D_0(q) = \left[c^2 \left(q_0^2 + \sum_{l=1}^{d_L} q_l^2 \right) + \sum_{n=d_L+1}^{d_M} q_n^2 + |\mathbf{M}|^2 \right]^{-1} \quad (4)$$

respectively, with the parameter c encoding the anisotropy in the bosonic dynamics, stemming from the anisotropic dispersion of the fermionic excitations.

Scaling. For the scaling analysis, we conveniently define a $(d_L + 1)$ -dimensional frequency-momentum vector $\mathbf{k} \equiv (k_0, k_1, \dots, k_{d_L})$ and d_M -dimensional momentum $\mathbf{K} \equiv (k_{d_L+1}, \dots, k_d)$, with the scaling dimensions $[\mathbf{K}] = 1$ and $[\mathbf{k}] = z_{\mathbf{k}}$. When the function ε_n from Eq. (1) depends on the n th power of its arguments in the d_M -dimensional hyperplane, as is the case for general WSMs (discussed shortly), the action in Eq. (2) is invariant under the tree-level scaling upon setting $z_{\mathbf{k}} = n$ at the non-interacting fixed point. The fermionic action yields $[\psi] = -[z_{\mathbf{k}}(d_L + 2) + d_M]/2$ as $[G_0^{-1}] = z_{\mathbf{k}}$. Furthermore, we have $[c] = 1 - z_{\mathbf{k}}$ and $[M] = 1$, leading to the scaling dimension of the bosonic field $[\phi^2] = -2 - [z_{\mathbf{k}}(d_L + 1) + d_M]$, since $[D_0^{-1}] = 2$. Then for the Yukawa term we find $[g_0^2] =$

arguments, δ_{ij} is the Kronecker delta-function, and v_l bears the dimension of Fermi velocity. For simplicity, we set $v_l = v = 1$ for all l . Short-ranged Hubbard-like interactions can trigger a symmetry breaking by generating a (multicomponent) mass term $\sum_{j=1}^{N_b} M_j \Upsilon_j$, where $M_j = \langle \Psi^\dagger \Upsilon_j \Psi \rangle$ and $\{\Upsilon_j\}$ is another set of mutually anticommuting Hermitian matrices such that $\{\Upsilon_i, \Upsilon_j\} = 2\delta_{ij}$ and $\{\Gamma_i, \Upsilon_j\} = 0$. The internal structure of fermionic spinors (Ψ^\dagger and Ψ) depends on the microscopic details, which we do not delve into here. Such an ordering leads to a fully and isotropic gapped state (insulator), where the magnitude of \mathbf{M} determines the condensation energy gain. The dimensionality of all Γ_j s and Υ_j s is $4N$.

Near the quantum critical point (QCP), relevant degrees of freedom are gapless nodal fermions and bosonic order parameter fluctuations, coupled via a Yukawa interaction. The effective imaginary time action reads

$2 - [z_{\mathbf{k}}(d_L - 1) + d_M]$, which is marginal on the line $z_{\mathbf{k}}(d_L - 1) + d_M = 2$, and passes through the point $(d_L, d_M) = (1, 2)$, representing the marginality condition in the non-Lorentz symmetric theory.

Interacting fixed points where the Yukawa coupling is dimensionful can then be reached by independently tuning the deviations from this marginal line in term of the ‘small’ parameters $\varepsilon_L = \bar{d}_L - d_L$ and $\varepsilon_M = \bar{d}_M - d_M$, where $z_{\mathbf{k}}(\bar{d}_L - 1) + \bar{d}_M = 2$. This is accomplished through dimensional regularization within the minimal subtraction scheme [13, 47], yielding the RG flow equation for the Yukawa coupling. On this line the quartic bosonic coupling is irrelevant for any $n > 1$ as $[u_0] = 4 - z_{\mathbf{k}}(d_L + 1) - d_M$, which we do not therefore consider in the following analysis. By contrast, a Lorentz symmetric theory is marginal at the point $(d_L, d_M) = (3, 0)$, where both g_0 and u_0 are marginal and the access to the nontrivial QCP is controlled by an $\varepsilon = 3 - d$ expansion.

Interacting WSM. With the stage being set, we proceed to capture the emergent quantum criticality in general WSMs, with their Hamiltonian given by

$$H_n(k_\perp, k_z) = \alpha_n k_\perp^n [\Gamma_1 C_n \phi_{\mathbf{k}} + \Gamma_2 S_n \phi_{\mathbf{k}}] + \Gamma_3 v_z k_z, \quad (5)$$

when they reside at the brink of axionic insulation, where $C_x = \cos(x)$ and $S_x = \sin(x)$. Mutually anticommuting Γ matrices are $\Gamma_1 = \tau_0 \otimes \sigma_1$, $\Gamma_2 = \tau_0 \otimes \sigma_2$, and $\Gamma_3 = \tau_3 \otimes \sigma_3$. Pauli matrices σ_μ (τ_μ) act on the orbital (valley) subspace, and $\phi_{\mathbf{k}} = \tan^{-1}(k_y/k_x)$. The parameters α_n and v_z are real and positive, with α_1 and

v_z (α_2) bearing the dimension of Fermi velocity (inverse mass). The bare fermionic propagator reads $G_0(\mathbf{k}, \mathbf{K}) = [ik_0 + H_n(k_x, k_y, k_z)]^{-1}$, where the corresponding momentum 2-vectors are $\mathbf{k} \equiv (k_0, k_z)$ and $\mathbf{K} \equiv (k_x, k_y)$.

For sufficiently strong interactions, WSMs with any n can undergo a QPT into a translational symmetry breaking axion insulator [46], which is two-component (XY) order with $N_b = 2$, and is represented by the mutually anticommuting matrices $\Upsilon_1 \equiv \Gamma_4 = \tau_1 \otimes \sigma_3$ and $\Upsilon_2 \equiv \Gamma_5 = \tau_2 \otimes \sigma_3$. These two matrices also anticommute with the Γ matrices in the Hamiltonian of the WSM [Eq. (5)]. Therefore, axionic insulator fully gaps out the nodal fermionic excitations. The corresponding effective single-particle Hamiltonian is

$$H_{\text{AI}} = |\mathbf{M}| [\Upsilon_1 \cos(\theta) + \Upsilon_2 \sin(\theta)]. \quad (6)$$

The U(1) Goldstone mode describing the fluctuations of θ is known as the axion field, and it couples with the external electromagnetic fields through the axion term $\theta \mathbf{E} \cdot \mathbf{B}$. In quantum crystals, θ describes the sliding mode.

RG analysis. The $4N$ -dimensional Γ and Υ matrices allow us to perform the RG analysis near the QCP associated to a general N_b -component insulating order parameter, with our ultimate focus near the axionic QCP. Before delving into such an exercise in general WSMs, we consider simple WSM with Lorentz invariance, $d_L = 3$, and $d_M = 0$ in Eq. (2). The coupled RG flow equations can then be readily obtained [48] and are given by

$$\frac{dg^2}{d\ell} = \varepsilon g^2 - \left(N + \frac{1}{N_f}\right) \frac{g^4}{8\pi^2}, \quad (7)$$

$$\frac{du}{d\ell} = \varepsilon u - \left(u - \frac{Ng^2}{N_f}\right) \frac{g^2}{4\pi^2} - \left(4 + \frac{N_b}{2}\right) \frac{u^2}{8\pi^2}, \quad (8)$$

which feature a nontrivial QCP for $d < 3$ ($\varepsilon > 0$) at $g_* \sim \varepsilon$ and $u_* \sim \varepsilon$. Here, $\ell \equiv -\ln \mu$ is the logarithm of the running RG scale and μ is the momentum scale. Such a QCP is characterized by the non-mean-field correlation length exponent, $\nu^{-1} = 2 - (N_b + 2)u_*/(16\pi^2) - Ng_*^2/(8\pi^2)$, and the anomalous dimensions of the fermionic and bosonic fields, $\eta_\psi = g_*^2/(16\pi^2 N_f)$ and $\eta_\phi = Ng_*^2/(8\pi^2)$, respectively, to the leading order in the ε expansion.

Next, we focus on 3D general WSMs and cast the inverse fermionic propagator as $G_0^{-1}(\mathbf{k}, \mathbf{K}) = i\Gamma_{13}[\mathbf{k} \cdot \boldsymbol{\gamma} + |\mathbf{K}|^n \hat{\mathbf{n}}_{\mathbf{k}} \cdot \boldsymbol{\Gamma}]$, where $\boldsymbol{\gamma} = (\Gamma_{13}, -\Gamma_{20})$, $\boldsymbol{\Gamma} = (\Gamma_{12}, -\Gamma_{11})$, $\Gamma_{ij} = \tau_i \otimes \sigma_j$, $\hat{\mathbf{n}}_{\mathbf{k}} = (\cos(n\phi), \sin(n\phi))$, and $\phi \equiv \phi_{\mathbf{k}}$. We perform the RG analysis in two steps. First, we calculate the bosonic self-energy diagram within the $\varepsilon_M = 2 - d_M \equiv \varepsilon$ expansion around the marginal condition $d_M = 2$, keeping $d_L = 1$ fixed. This procedure explicitly takes into account the anisotropy of the fermionic dispersion [36]. The resulting dressed bosonic propagator is obtained by resumming the dominant random phase approximation processes [Fig. 1(a)], eliminating the putative infrared (IR) divergences in the limit $c \rightarrow 0$, which takes the form [49]

$$D^{-1}(\mathbf{q}, \mathbf{Q}) = N \left(|\mathbf{Q}|^2 + g^2 A_n |\mathbf{q}|^{2/n} \right), \quad (9)$$

where $g \equiv g_0 \mu^{(d_M - 2)/2}$ is the dimensionless Yukawa coupling. Upon setting the bosonic mass to zero, we find

$$A_n = -\frac{1}{(2\pi)^2} \int_0^\infty dz \int_0^1 dx \frac{x^2 - z^n}{x(x-1) - z^n}. \quad (10)$$

At an intermediate momentum scale μ , the action from Eq. (2) then takes the form [49]

$$S = \sum_{p=1}^{N_f} \left[i \int_{\mathbf{k}} \psi_{p,k}^\dagger \Gamma_{13} [\mathbf{k} \cdot \boldsymbol{\gamma} + |\mathbf{K}|^n \hat{\mathbf{n}}_{\mathbf{k}} \cdot \boldsymbol{\Gamma}] \psi_{p,k} + \frac{g\mu^{\frac{2-d_M}{2}}}{\sqrt{N_f}} \int_{\mathbf{k}, \mathbf{q}} \psi_{p,k+q}^\dagger \tilde{\Phi}_q \psi_{p,k} \right] + \frac{1}{8} \int_{\mathbf{q}} (|\mathbf{Q}|^2 + M^2) \text{tr} \left\{ \tilde{\Phi}_q \tilde{\Phi}_q \right\}, \quad (11)$$

where we keep only the marginal and relevant terms close to $d_L = 1$ and $d_M = 2$, and $\tilde{\Phi}_q = \sum_{j=1}^{N_b} \phi_j(q) \Upsilon_j$.

This procedure brings the action into a renormalizable form which in the second step we treat by adding counterterms. After setting the renormalized bosonic mass M to zero (critical plane), the renormalized action reads

$$S_r = i \int_{\mathbf{k}} \psi_{\mathbf{k}}^\dagger [\mathcal{Z}_1 \mathbf{k} \cdot \boldsymbol{\gamma} + \mathcal{Z}_2 |\mathbf{K}|^n \hat{\mathbf{n}}_{\mathbf{k}} \cdot \boldsymbol{\Gamma}] \psi_{\mathbf{k}} + \frac{1}{8} \int_{\mathbf{q}} \mathcal{Z}_3 |\mathbf{Q}|^2 \text{tr} \left\{ \tilde{\Phi}_q \tilde{\Phi}_q \right\} + g\mu^{(3-d)/2} \mathcal{Z}_4 \int_{\mathbf{k}, \mathbf{q}} \psi_{\mathbf{k}+\mathbf{q}}^\dagger \tilde{\Phi}_q \psi_{\mathbf{k}}. \quad (12)$$

To the leading order in the ε expansion, $\mathcal{Z}_n = 1 + Z_n/\varepsilon$ are renormalization factors, absorbing the ensuing divergences in the $\varepsilon = 2 - d_M$ expansion close to $d_M = 2$. We emphasize that here we use the dressed (re-

summed) damped bosonic propagator, given by Eq. (9), to regulate the putative IR divergences in the fermionic self-energy [Fig. 1(b)] and vertex [Fig. 1(c)] corrections in the limit $c \rightarrow 0$ [36]. The explicit calcula-

tion of the renormalization factors from the fermionic self-energy yields $Z_1 = -N_b g^2 / (8\pi^2 N N_f)$ and $Z_2 = (n N_b g^2 / (8\pi^2 N N_f)) \ln(C_n g^2)$, where C_n is a real function of n [49]. From the bosonic self-energy, we find $Z_3 = -N n^2 g^2 / (4\pi^2)$. The Yukawa vertex correction gives $Z_4 = (N_b - 2)(n g^2 / 8\pi^2 N N_f) \ln(A_n g^2)$, which vanishes for the axionic XY order parameter ($N_b = 2$) [6].

The relations between the bare (with the subscript ‘ B ’) and renormalized quantities are given by

$$\begin{aligned} \mathbf{k}_B &= Z_{\mathbf{k}}^{-1} \mathbf{k}, \mathbf{K}_B = \mathbf{K}, \psi_B = \sqrt{Z_\psi} \psi, \phi_B = \sqrt{Z_\phi} \phi, \\ g_0 \equiv g_B &= \mu^{\frac{2-d_M}{2}} \frac{Z_{\mathbf{k}}^4 Z_4}{Z_\psi \sqrt{Z_\phi}} g, \end{aligned} \quad (13)$$

where $Z_{\mathbf{k}} = Z_2 / Z_1$, $Z_\psi = Z_2 Z_{\mathbf{k}}^2$ and $Z_\phi = Z_3 Z_{\mathbf{k}}^2$. The anisotropy exponent $z_{\mathbf{k}}$ and the anomalous dimensions (η_ψ and η_ϕ) of the fields are defined as

$$z_{\mathbf{k}} = n - \frac{\partial \ln Z_{\mathbf{k}}}{\partial \ln \mu}, \eta_\psi = \frac{1}{2} \frac{\partial \ln Z_\psi}{\partial \ln \mu}, \eta_\phi = \frac{1}{2} \frac{\partial \ln Z_\phi}{\partial \ln \mu}. \quad (14)$$

The RG flow equation for the Yukawa coupling is obtained from the condition of the bare coupling being fixed, $\partial g_B / \partial \ln \mu = 0$. After solving this system of equations and using the obtained values of the Z factors [49], we find the anomalous dimensions and the RG flow equation for the Yukawa coupling, which we analyze next.

Results. The RG flow equation for the Yukawa coupling reads as

$$\frac{dg^2}{dl} = \varepsilon g^2 - \frac{g^4}{4\pi^2} \left[N n^2 + \frac{N_b + n(N_b - 2) \ln(e A_n g^2)}{N N_f} \right]. \quad (15)$$

with A_n given in Eq. (10). Therefore, the noninteracting fixed point at $g_*^2 = 0$ is IR stable for any $N_b \leq 2$ when $\varepsilon = 0$. On the other hand, a IR stable fixed point $g_*^2 \sim \varepsilon$ is obtained for any N_b and $d_M < 2$. In the limit $\varepsilon \ll 1$ and $N_f \gg 1$, the XY QCP ($N_b = 2$) is located at

$$g_*^2 = \frac{4\pi^2}{N n^2} \left(1 - \frac{2}{N^2 n^2 N_f} \right) \varepsilon, \quad (16)$$

where we find

$$z_{\mathbf{k}} = n + \frac{\varepsilon \ln \varepsilon}{N^2 n N_f}, \eta_\psi = -\frac{3\varepsilon \ln \varepsilon}{2N^2 n N_f}, \eta_\phi = \frac{\varepsilon}{2} - \frac{\varepsilon \ln \varepsilon}{N^2 n N_f} \quad (17)$$

and the correlation length exponent (ν), obtained from the relevant RG flow of the bosonic mass (the tuning parameter for the QPT), is given by

$$\nu^{-1} \equiv 2 - 2\eta_\phi = 2 - \varepsilon + \frac{2}{N^2 n N_f} \varepsilon \ln \varepsilon. \quad (18)$$

Therefore, the axionic QCP in an interacting general WSM is located at $g_*^2 = 0$. At this fixed point, all the exponents ultimately assume mean-field values, namely $z_{\mathbf{k}} = n$, $\eta_\psi = 0$, $\eta_\phi = 0$, and $\nu = 1/2$. However, these

mean-field values are approached only logarithmically slowly as a function of the running scale (μ), yielding a marginal Fermi liquid at the axionic QCP. Therefore, the marginal Fermi liquid showcases logarithmic corrections to the scaling of various physical observables as function of temperature (T) or frequency (ω), playing the role of the running scale, in contrast to those in noninteracting systems, displaying power-law scaling, discussed next.

For example, the specific heat (C_v) and compressibility (κ) scale as $T^{1+d_M/z_{\mathbf{k}}}$ and $T^{d_M/z_{\mathbf{k}}}$, respectively, and the Grüneisen ratio scales as $\Gamma_G \sim T^{-(2+d_M/z_{\mathbf{k}})}$. The band curvature of the fermionic dispersion is modified according to $[k_z^2 + k_\perp^{2z_{\mathbf{k}}}]^{1/2}$. While the spectral density function near the Weyl points scales as $\mathcal{A}(\omega) \sim \omega^{-1+2\eta_\psi}$, the dynamic structure factor for the order parameter fluctuations goes as $\mathcal{S}(\omega) \sim \omega^{-2+2\eta_\phi}$. The scaling of the zero temperature longitudinal optical conductivity at finite frequency can be obtained from the gauge invariance of the current-current correlator, yielding $\sigma_{zz} \sim \omega^{-1+(2-\varepsilon)/z_{\mathbf{k}}}$ and $\sigma_{jj} \sim \omega^{1-\varepsilon/z_{\mathbf{k}}}$ for $j = x$ and y .

Before closing this section, we briefly comment on the structure of the fixed point for $N_b \neq 2$. Within the realm of the ε expansion, there exists an IR stable fixed point at $g_*^2 = a/W_s(a A_n e^b)$, where $a = 4\pi^2 N N_f \varepsilon / [n(N_b - 2)]$, $b = (N^2 n^2 N_f + N_b + n(N_b - 2)) / [n(N_b - 2)]$. Here $W_s(x)$ is the product of the logarithm on the s th branch, and for $N_b = 1$ ($N_b \geq 3$), the parameter $s = -1$ ($s = 0$) [49]. As $g_*^2 \sim \varepsilon$, this fixed point also manifests Gaussian quantum criticality. However, even if we set $\varepsilon = 0$ in Eq. (15), there exists an IR stable fixed point for $N_b \geq 3$ at

$$g_*^2 = \frac{1}{A_n} \exp \left[-\frac{N N_f}{n(N_b - 2)} \left(N n^2 + \frac{N_b + n(N_b - 2)}{N N_f} \right) \right] \quad (19)$$

which is beyond the territory of the ε expansion.

Summary and discussions. To summarize, here we expose the quantum critical properties of interacting 3D WSMs (both simple and general) when they reside at the brink of axionic insulation, triggered by suitable short-range Hubbard-like interactions. While in such a situation traditional field theoretic RG approach can be applied in simple WSMs, our proposed field theoretic approach is tailored to address similar quests in generic non-Lorentz symmetric interacting semimetals that encompasses general WSMs. Both methods, nonetheless, predict that the WSM to axion insulator QPT is Gaussian in nature, and the critical exponents ultimately acquire their mean-field values. The resulting marginal Fermi liquid, residing around the underlying QCP, thus features logarithmic corrections to the scaling of thermodynamic and transport quantities as a function of temperature and frequency, respectively. Strong Hubbard-like interactions can make WSMs susceptible to the nucleation of rotational symmetry-breaking nematic orders, which, in simple (general) WSMs, shift the location of (split) the Weyl nodes [46, 50]. Future investigations will unfold the

underlying critical properties around such orderings.

Signatures of the axionic insulation in Weyl materials have remained elusive so far, unless they are placed in strong magnetic fields [51]. Application of external magnetic fields quenches the kinetic energy and gives birth to Landau levels that are dispersive in the field direction. The resulting finite density of states triggers the onset of axion insulator even for infinitesimal interactions, following the magnetic catalysis mechanism [52, 53]. However, WSMs realized on strongly correlated quantum crystals, such as 227 pyrochlore iridates with multipolar magnetic orders [54–58] and Kondo materials [59–61], can be the ideal place to harness such exotic insulating ground state and hallmarks of emergent marginal Fermi liquids in terms of the logarithmic scaling corrections of physical observables, predicted in this work.

Acknowledgments. This work was supported by ANID/ACT210100 (G.M., R.S.-G., and V.J.), the Swedish Research Council Grant No. VR 2019-04735 (V.J.), Fondecyt (Chile) Grants No. 1241033 (R.S.-G.) and No. 1230933 (V.J.). B.R. was supported by NSF CAREER Grant No. DMR-2238679 and is grateful to Institute for Solid State Physics, University of Tokyo where a part of this work was performed for their hospitality.

-
- [1] L. D. Landau, The theory of a Fermi liquid, *Sov. Phys. JETP* **3**, 920 (1957).
- [2] S. Sachdev, *Quantum Phase Transitions* (Cambridge University Press, Cambridge, England, 2011).
- [3] M. A. Metlitski and S. Sachdev, Quantum phase transitions of metals in two spatial dimensions. I. Ising-nematic order, *Phys. Rev. B* **82**, 075127 (2010).
- [4] M. A. Metlitski and S. Sachdev, Quantum phase transitions of metals in two spatial dimensions. II. Spin density wave order, *Phys. Rev. B* **82**, 075128 (2010).
- [5] D. Dalidovich and S.-S. Lee, Perturbative non-Fermi liquids from dimensional regularization, *Phys. Rev. B* **88**, 245106 (2013).
- [6] S. Sur and S.-S. Lee, Anisotropic non-Fermi liquids, *Phys. Rev. B* **94**, 195135 (2016).
- [7] Y. Schattner, S. Lederer, S. A. Kivelson, and E. Berg, Ising Nematic Quantum Critical Point in a Metal: A Monte Carlo Study, *Phys. Rev. X* **6**, 031028 (2016).
- [8] X. Y. Xu, K. Sun, Y. Schattner, E. Berg, and Z. Y. Meng, Non-Fermi Liquid at $(2 + 1)$ D Ferromagnetic Quantum Critical Point, *Phys. Rev. X* **7**, 031058 (2017).
- [9] W. Kohn and J. M. Luttinger, New Mechanism for Superconductivity, *Phys. Rev. Lett.* **15**, 524 (1965).
- [10] M. A. Baranov, A. V. Chubukov, and M. Yu. Kagan, Superconductivity and superfluidity in Fermi systems with repulsive interactions, *Int. J. Mod. Phys. B* **06**, 2471 (1992).
- [11] R. Shankar, Renormalization-group approach to interacting fermions, *Rev. Mod. Phys.* **66**, 129 (1994).
- [12] N. P. Armitage, E. J. Mele, and A. Vishwanath, Weyl and Dirac semimetals in three-dimensional solids, *Rev. Mod. Phys.* **90**, 015001 (2018).
- [13] J. Zinn-Justin, *Quantum Field Theory and Critical Phenomena* (Oxford University Press, Oxford, England, 2002).
- [14] B. Rosenstein, H.-L. Yu, and A. Kovner, Critical exponents of new universality classes, *Phys. Lett. B* **314**, 381 (1993).
- [15] J. Gracey, Computation of critical exponent η at $O(1/N^3)$ in the four-Fermi model in arbitrary dimensions, *Int. J. Mod. Phys. A* **09**, 727 (1994).
- [16] M. Vojta, Y. Zhang, and S. Sachdev, Quantum Phase Transitions in d -Wave Superconductors, *Phys. Rev. Lett.* **85**, 4940 (2000).
- [17] M. Moshe and J. Zinn-Justin, Quantum field theory in the large N limit: a review, *Physics Reports* **385**, 69 (2003).
- [18] S.-S. Lee, Emergence of supersymmetry at a critical point of a lattice model, *Phys. Rev. B* **76**, 075103 (2007).
- [19] I. F. Herbut, V. Juričić, and B. Roy, Theory of interacting electrons on the honeycomb lattice, *Phys. Rev. B* **79**, 085116 (2009).
- [20] I. F. Herbut, V. Juričić, and O. Vafek, Relativistic Mott criticality in graphene, *Phys. Rev. B* **80**, 075432 (2009).
- [21] B. Roy, Multicritical behavior of $\mathbb{Z}_2 \times O(2)$ Gross-Neveu-Yukawa theory in graphene, *Phys. Rev. B* **84**, 113404 (2011).
- [22] N. Zerf, C.-H. Lin, and J. Maciejko, Superconducting quantum criticality of topological surface states at three loops, *Phys. Rev. B* **94**, 205106 (2016).
- [23] B. Roy, M. P. Kennett, K. Yang, and V. Juričić, From Birefringent Electrons to a Marginal or Non-Fermi Liquid of Relativistic Spin-1/2 Fermions: An Emergent Superuniversality, *Phys. Rev. Lett.* **121**, 157602 (2018).
- [24] S. Sorella and E. Tosatti, Semi-Metal-Insulator Transition of the Hubbard Model in the Honeycomb Lattice, *Europhys. Lett.* **19**, 699 (1992).
- [25] F. F. Assaad and I. F. Herbut, Pinning the Order: The Nature of Quantum Criticality in the Hubbard Model on Honeycomb Lattice, *Phys. Rev. X* **3**, 031010 (2013).
- [26] F. Parisen Toldin, M. Hohenadler, F. F. Assaad, and I. F. Herbut, Fermionic quantum criticality in honeycomb and π -flux Hubbard models: Finite-size scaling of renormalization-group-invariant observables from quantum Monte Carlo, *Phys. Rev. B* **91**, 165108 (2015).
- [27] Y. Otsuka, S. Yunoki, and S. Sorella, Universal Quantum Criticality in the Metal-Insulator Transition of Two-Dimensional Interacting Dirac Electrons, *Phys. Rev. X* **6**, 011029 (2016).
- [28] Z.-X. Li, Y.-F. Jiang, and H. Yao, Fermion-sign-free Majorana-quantum-Monte-Carlo studies of quantum critical phenomena of Dirac fermions in two dimensions, *New J. Phys.* **17**, 085003 (2015).
- [29] H.-M. Guo, L. Wang, and R. T. Scalettar, Quantum phase transitions of multispecies Dirac fermions, *Phys. Rev. B* **97**, 235152 (2018).
- [30] T. C. Lang and A. M. Läuchli, Quantum Monte Carlo Simulation of the Chiral Heisenberg Gross-Neveu-Yukawa Phase Transition with a Single Dirac Cone, *Phys. Rev. Lett.* **123**, 137602 (2019).
- [31] Y. Huang, H. Guo, J. Maciejko, R. T. Scalettar, and S. Feng, Antiferromagnetic transitions of Dirac fermions in three dimensions, *Phys. Rev. B* **102**, 155152 (2020).
- [32] T. Sato, Z. Wang, Y. Liu, D. Hou, M. Hohenadler, W. Guo, and F. F. Assaad, Simulation of fermionic and bosonic critical points with emergent $SO(5)$ symmetry,

- Phys. Rev. B* **108**, L121111 (2023).
- [33] V. Juričić and B. Roy, Yukawa-Lorentz symmetry in non-Hermitian Dirac materials, *Commun. Phys.* **7**, 169 (2024).
- [34] S. A. Murshed and B. Roy, Quantum electrodynamics of non-hermitian dirac fermions, *Journal of High Energy Physics* **2024**, 143 (2024).
- [35] X.-J. Yu, Z. Pan, L. Xu, and Z.-X. Li, Non-Hermitian Strongly Interacting Dirac Fermions, *Phys. Rev. Lett.* **132**, 116503 (2024).
- [36] S. Sur and B. Roy, Unifying Interacting Nodal Semimetals: A New Route to Strong Coupling, *Phys. Rev. Lett.* **123**, 207601 (2019).
- [37] G. Xu, H. Weng, Z. Wang, X. Dai, and Z. Fang, Chern Semimetal and the Quantized Anomalous Hall Effect in HgCr_2Se_4 , *Phys. Rev. Lett.* **107**, 186806 (2011).
- [38] C. Fang, M. J. Gilbert, X. Dai, and B. A. Bernevig, Multi-Weyl Topological Semimetals Stabilized by Point Group Symmetry, *Phys. Rev. Lett.* **108**, 266802 (2012).
- [39] B.-J. Yang and N. Nagaosa, Classification of stable three-dimensional Dirac semimetals with nontrivial topology, *Nat. Commun.* **5**, 4898 (2014).
- [40] S.-M. Huang, S.-Y. Xu, I. Belopolski, C.-C. Lee, G. Chang, T.-R. Chang, B. Wang, N. Alidoust, G. Bian, M. Neupane, D. Sanchez, H. Zheng, H.-T. Jeng, A. Bansil, T. Neupert, H. Lin, and M. Z. Hasan, New type of Weyl semimetal with quadratic double Weyl fermions, *Proc. Natl. Acad. Sci. USA* **113**, 1180 (2016).
- [41] Q. Liu and A. Zunger, Predicted Realization of Cubic Dirac Fermion in Quasi-One-Dimensional Transition-Metal Monochalcogenides, *Phys. Rev. X* **7**, 021019 (2017).
- [42] Z. Wang and S.-C. Zhang, Chiral anomaly, charge density waves, and axion strings from Weyl semimetals, *Phys. Rev. B* **87**, 161107 (2013).
- [43] J. Maciejko and R. Nandkishore, Weyl semimetals with short-range interactions, *Phys. Rev. B* **90**, 035126 (2014).
- [44] Y. Wang and P. Ye, Topological density-wave states in a particle-hole symmetric Weyl metal, *Phys. Rev. B* **94**, 075115 (2016).
- [45] M. Laubach, C. Platt, R. Thomale, T. Neupert, and S. Rachel, Density wave instabilities and surface state evolution in interacting Weyl semimetals, *Phys. Rev. B* **94**, 241102 (2016).
- [46] B. Roy, P. Goswami, and V. Juričić, Interacting weyl fermions: Phases, phase transitions, and global phase diagram, *Phys. Rev. B* **95**, 201102 (2017).
- [47] M. E. Peskin and D. V. Schroeder, *An Introduction to Quantum Field Theory* (CRC Press, London, England, 2019).
- [48] B. Roy, V. Juričić, and I. F. Herbut, Quantum superconducting criticality in graphene and topological insulators, *Phys. Rev. B* **87**, 041401 (2013).
- [49] See Supplemental Material at XXX-XXXX for the details of the RG calculation.
- [50] S.-K. Jian and H. Yao, Fermion-induced quantum critical points in three-dimensional Weyl semimetals, *Phys. Rev. B* **96**, 155112 (2017).
- [51] J. Gooth, B. Bradlyn, S. Honnali, C. Schindler, N. Kumar, J. Noky, Y. Qi, C. Shekhar, Y. Sun, Z. Wang, B. A. Bernevig, and C. Felser, Axionic charge-density wave in the Weyl semimetal $(\text{TaSe}_4)_2\text{I}$, *Nature (London)* **575**, 315 (2019).
- [52] B. Roy and J. D. Sau, Magnetic catalysis and axionic charge density wave in Weyl semimetals, *Phys. Rev. B* **92**, 125141 (2015).
- [53] X. Li, B. Roy, and S. Das Sarma, Weyl fermions with arbitrary monopoles in magnetic fields: Landau levels, longitudinal magnetotransport, and density-wave ordering, *Phys. Rev. B* **94**, 195144 (2016).
- [54] X. Wan, A. M. Turner, A. Vishwanath, and S. Y. Savrasov, Topological semimetal and Fermi-arc surface states in the electronic structure of pyrochlore iridates, *Phys. Rev. B* **83**, 205101 (2011).
- [55] Y. Yamaji and M. Imada, Metallic Interface Emerging at Magnetic Domain Wall of Antiferromagnetic Insulator: Fate of Extinct Weyl Electrons, *Phys. Rev. X* **4**, 021035 (2014).
- [56] W. Witczak-Krempa, G. Chen, Y. B. Kim, and L. Balents, Correlated Quantum Phenomena in the Strong Spin-Orbit Regime, *Annu. Rev. Condens. Matter Phys.* **5**, 57 (2014).
- [57] P. Goswami, B. Roy, and S. Das Sarma, Competing orders and topology in the global phase diagram of pyrochlore iridates, *Phys. Rev. B* **95**, 085120 (2017).
- [58] K. Ladovrechis, T. Meng, and B. Roy, Competing magnetic orders and multipolar Weyl fermions in 227 pyrochlore iridates, *Phys. Rev. B* **103**, L241116 (2021).
- [59] H.-H. Lai, S. E. Grefe, S. Paschen, and Q. Si, Weyl-Kondo semimetal in heavy-fermion systems, *Proc. Natl. Acad. Sci. USA* **115**, 93 (2017).
- [60] L. Chen, C. Setty, H. Hu, M. G. Vergniory, S. E. Grefe, L. Fischer, X. Yan, G. Eguchi, A. Prokofiev, S. Paschen, J. Cano, and Q. Si, Topological semimetal driven by strong correlations and crystalline symmetry, *Nat. Phys.* **18**, 1341 (2022).
- [61] S. Dzsaber, L. Prochaska, A. Sidorenko, G. Eguchi, R. Svagera, M. Waas, A. Prokofiev, Q. Si, and S. Paschen, Kondo Insulator to Semimetal Transformation Tuned by Spin-Orbit Coupling, *Phys. Rev. Lett.* **118**, 246601 (2017).